Electrochimica Acta 111 (2013) 797–801

Contents lists available at ScienceDirect

Electrochimica Acta

journal homepage: www.elsevier.com/locate/electacta

Material characteristics and electrochemical performance of Sn-doped ZnO spherical-particle photoanode for dye-sensitized solar cells

Haohao Wang [a], Ripon Bhattacharjee [b], I-Ming Hung [b,*], Langkai Li [a], Renjie Zeng [a]

[a] Department of Materials Science and Engineering, Xiamen University, Xiamen 361005, People's Republic of China
[b] Department of Chemical Engineering and Materials Science, Yuan Ze University, Taoyuan 320, Taiwan

ARTICLE INFO

Article history:
Received 17 May 2013
Received in revised form 28 July 2013
Accepted 28 July 2013
Available online xxx

Keywords:
Dye-sensitized solar cells
ZnO
Sn element
Spherical particle

ABSTRACT

The aim of this study was to examine the effects of Sn element on the characteristics and electrochemical properties of ZnO spherical-particle used as dye sensitized solar cells (DSSCs) photoanode. Spherical nanoparticles were synthesized via a polyol mediated precipitation method and four concentrations of Sn–Zn = 0, 3, 4, and 5 wt.% of photoelectrodes were prepared. Their structures, morphologies, photovoltaic performances and electrochemical properties were studied through XRD, SEM, TEM, *J–V*, IPCE and EIS. It was observed that the efficiency of dye-sensitized solar cells increased with the addition of Sn element and the SZO4 (Sn–Zn = 4 wt.%) based DSSC had the highest power energy conversion efficiency of 0.80%, which is greatly increased compared to that of the DSSC based on ZnO (0.28%).

1. Introduction

Dye-sensitized solar cells (DSSCs), which are regarded as the third generation of solar PV devices owing to their potential low-cost of manufacturing, non-toxicity and environment-friendliness, have been deeply studied since Grätzel and coworkers put it forward for the first time in 1991 [1]. A DSSC is a photoelectrochemical system, in which the photoelectrode plays a vitally important role. ZnO is an attractive electrode material and has drawn considerable attention due to its large energy band gap (3.37 eV) and high electron mobility (115–155 $cm^2\ V^{-1}\ s^{-1}$) [2].

In order to improve the DSSC efficiency, much work has been reported on modifying ZnO by doping with various dopants such as Sn [3], Al [4], Ga [5], F [6], In [7] and Cu [8]. Metal doping is the effective procedure to improve the electrochemical performance of ZnO due to modify the grain size, orientation and the conductivity of the ZnO nanostructures. Several researches reported that the Sn-doped ZnO thin films for enhancing the electrical and optical properties [9] that due to the effect of Sn doping on the grain size, crystallinity, microstructure, optical and structural properties of ZnO thin film [10–12]. Recently, Ameen et al. [3] investigated the structure of Sn-doped ZnO by X-ray photoelectron spectroscopy (XPS), X-ray diffraction (XRD), Raman and ultra violet-diffused reflectance (UV-DRS) in detail, it was found that the Sn-ions into ZnO nanostructures to replace the Zn-ions and clearly observed that the grain size decreased from ~143.9 nm to ~82.2 nm and the electrochemical performance improved. On the other hand, different morphologies significantly affect the DSSC efficiency. Therefore, lots of researches have synthetized varieties of ZnO nanostructures for DSSC photoelectrodes, such as nanorods [13], nanoflowers [14], nanotubes [15], nanowires [16] and nanofibers [17]. The spherical nanocrystallite aggregates are believed to possess many superior properties, including large specific surface area, effective scattering property and the facilitating electrolyte passing through large pores between aggregated particles [18]. Therefore, it is expected that this spherical structure can provide large dye adsorption amount and increase the DSSC efficiency [19].

In this study, ZnO and Sn–ZnO (SZO) spherical nanoparticles have successfully been synthesized by hydrolysis of zinc salt in a polyol medium [20,21]. Effects of different Sn element concentration on the material characters of ZnO and the performance of DSSCs were investigated in detail. The results show that the DSSCs based on SZO photoelectrodes exhibit a better efficiency compared to that of DSSC with ZnO photoelectrode.

2. Experimental details

2.1. Preparation of ZnO and SZO films

ZnO and Sn–ZnO (SZO) sample aggregates were synthesized via a polyol mediated precipitation method similar to that reported by Jezequel et al. [20]. Mixing zinc acetate dehydrate ($Zn(CH_3COO)_2{\cdot}2H_2O$, J.T. Baker) and tin tetrachloride ($SnCl_4$, Alfa

* Corresponding author. Tel.: +886 3 4638800x2569, fax: +886 3 4630634, +886 3 4559373.
E-mail address: imhung@saturn.yzu.edu.tw (I.-M. Hung).

0013-4686/$ – see front matter © 2013 Elsevier Ltd. All rights reserved.
http://dx.doi.org/10.1016/j.electacta.2013.07.199

Aesar) in different concentrations of Sn–Zn = 3, 4, and 5 wt.%, which are designated as SZO3, SZO4, SZO5. The mixture in diethylene glycol (DEG, Alfa Aesar) was rapidly heated to 160 °C and then kept at this temperature for 2 h until a milk-like suspension was formed. After the obtained colloid solution cooled to room temperature, the colloid was concentrated by a sequential treatment of centrifugation (7000 rpm for 5 min). The precipitates were washed with deionized water and ethanol several times respectively, and dried overnight at 80 °C. The precipitates were finally dispersed in ethanol with a concentration of 0.5 M and then ultrasonicated for 20 min to obtain a final colloidal suspension solution. The solution was spin-coated onto FTO glass (exposure area of 0.25 cm^2) for 30 s at 3000 rpm and annealed at 350 °C for 1 h to obtain the photoelectrode samples.

2.2. Dye-sensitized solar cell fabrication

0.5 mM ethanolic solution of the ruthenium complex *cis*-bis (2, 2-bipyridyl-4-dicarboxylato)-ruthenium(II)–bis-tetrabutylammonium (N719, Everlight Chemical Industrial Co.) was heated to 50 °C for 1 h. Photoelectrode samples were heated at 100 °C for 1 h and then immersed into dye in the dark place for 30 min. After 30 min of dye adsorption, the sensitized samples were rinsed with acetonitrile to remove excess dye from the surface and were dried at 70 °C for 30 min. The sensitized electrodes were assembled in a typical sandwich-type cell. The cell was covered with platinized ITO glass incorporating two drilled holes. Surlyn polymer with a thickness of 15 μm was used as the spacer. An Eversolar E5A (Everlight Chemical Industrial Co.), was used as the electrolyte, and injected into the space via the hole in the counter electrode. Finally, drill holes were sealed using Surlyn hot-melt polymer.

2.3. Characterization and photo-electrochemical measurements

The morphologies of samples were observed using scanning electron microscopes (FE-SEM, JEOL, JSM-6701F) and a high-resolution transmission electron microscopy (HR-TEM, JEOL, JEM-2100). Phase analyses were performed through X-ray diffraction (XRD, Shimadzu LabX, XRD-6000) with Cu Kα radiation (λ = 1.54056 Å) using an automated X-ray diffractometer. The photocurrent-voltage characteristics of the DSSCs were measured with Jiehan 5500 Photovoltaic Analyzer under a solar simulator (Yamashita Denso YSS-50A, AM 1.5, 100 mW cm^{-2}). The active area of the resultant cell exposed to light was 0.25 cm^2. A computer-controlled Keithley 2400 SourceMeter was employed to collect the current–voltage curves. The electrochemical impedance spectra were measured with an impedance analyzer (Solartron, 1255B) connected with a potentiostat (Solartron, 1287) at a frequency range from 0.1 Hz to 1 MHz with AC amplitude of 10 mV under the open-circuit status and light irradiation. The incident photo to current conversion efficiency (IPCE) of DSSCs was measured by a Keithley model 2000 SourceMeter under short circuit conditions using monochromatic light. The adsorption spectrum of the desorbed dye solution was measured using a UV–vis spectrophotometer (GBC Cintra 202).

3. Results and discussion

3.1. Structure and morphology of ZnO and SZO SNs

The structure and crystallinity of ZnO and SZO powders were analyzed by XRD patterns as shown in Fig. 1. The diffraction patterns of Fig. 1(a) were obtained at 2θ = 20–70° with the scanning speed of 2°/min. All diffraction peaks for ZnO and SZO photoelectrodes can be readily indexed as hexagonal wurtzite ZnO (JCPDS, No.36-1451) without any impurity phase. There is no SnO or other second phase was observed. Fig. 1(b) show the diffraction patterns of samples were obtained at 2θ = 35–38° with the low scanning speed of 0.05°/min. The peak corresponds to the (1 0 1) plane. The nanocrystallite size estimated from the full width at half maximum (FWHM) of the (1 0 1) peak according to the Debye–Scherrer formula and revealed that the nanocrystallites of ZnO and SZO were about 14–16 nm.

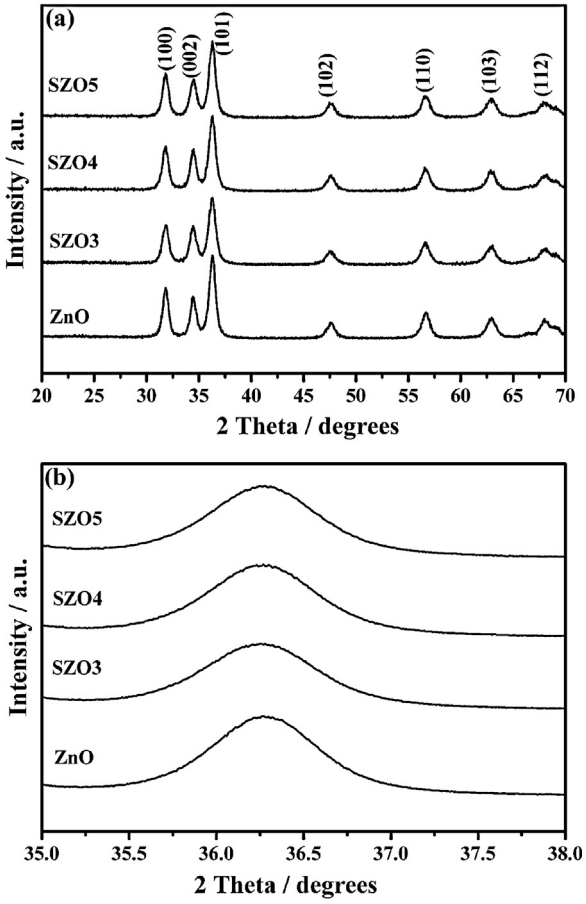

Fig. 1. XRD spectra of ZnO and SZO powders with (a) the scanning speed of 2°/min at 2θ = 20–70° and (b) the scanning speed of 0.05°/min at 2θ = 35–38°.

The FE-SEM micrographs of the ZnO and SZO powders were shown in Fig. 2 and the insets are corresponding particle size distributions. Uniform and highly aggregated submicron spherical particles were observed for all samples. About 84% particles are in the range of 500–700 nm for ZnO. About 83%, 86%, and 80% are in the range of 92–225 nm, 59–155 nm, and 71–175 nm for SZO3, SZO4, and SZO5, respectively. Apparently, the particle size of SZO powders is smaller than that of ZnO. On the other hand, it was found that the surface of ZnO is smooth; however, the surface of SZO is rough. It was expected that more amount of dye could be adsorbed on the surface of SZO powders. TEM was used to observe the morphology of ZnO and SZO nanocrystallites. Fig. 3 shows the TEM images of ZnO and SZO powders and the insets are the corresponding high magnification images. The images show that the aggregated spherical particle size of ZnO is much larger than that of SZO samples. These spherical particles were aggregated from 12 to 17 nm nanocrystallites, which were shown in the inserts. These results are highly consistent with the result observed from FE-SEM and calculated according to the Debye–Scherrer formula. From the result of XRD and FE-SEM, it was found that the crystallite of SZO is much smaller than that of ZnO, it was suggested that the Zn was easily substituted by Sn-ions in hydrothermal process due to the

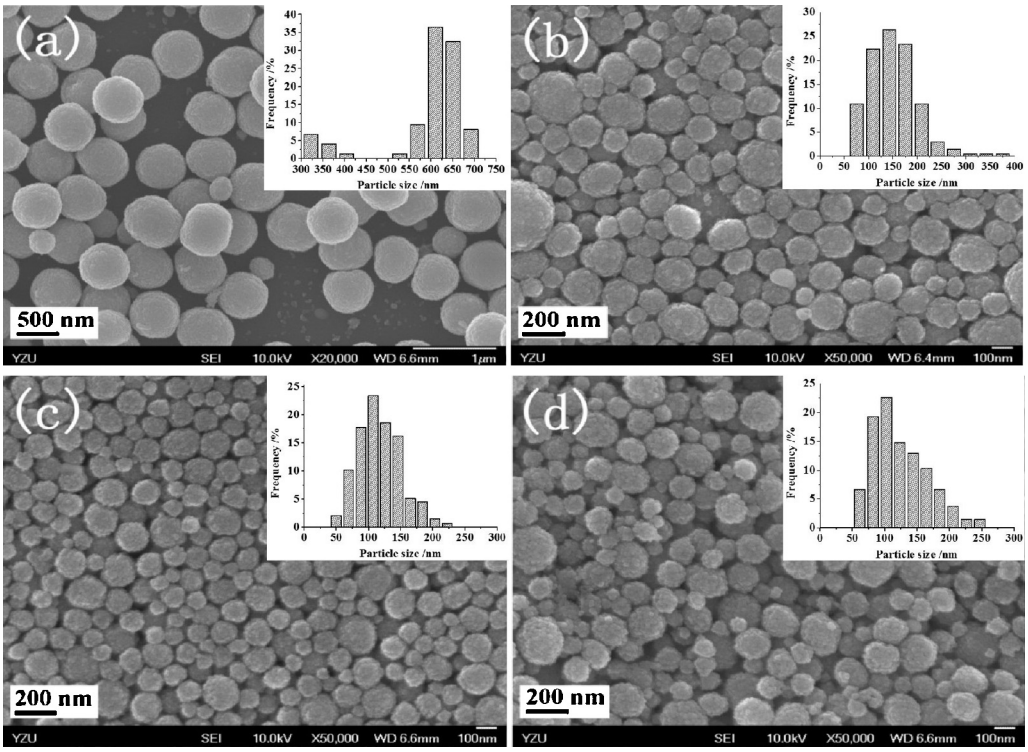

Fig. 2. FE-SEM micrographs of (a) ZnO, (b) SZO3, (c) SZO4, and (d) SZO5 powders. The insets are particle size distributions of the corresponding samples.

lesser radii of Sn than Zn [3]. The Sn element into the ZnO matrix structure decreased the growth rate of crystallite/grain of ZnO. This similar phenomenon was observed in doped ZnO research [3–5].

3.2. Photovoltaic performance

In order to study the photoelectrochemical performance of the DSSCs based on the ZnO and SZO photoanodes, the photovoltaic properties were measured under the AM 1.5 sunlight illumination ($100\,mW\,cm^{-2}$) from a Xenon lamp. The *J–V* curves of DSSCs are depicted in Fig. 4(a) and the corresponding results are summarized in Table 1. SZO photoanodes show higher efficiency of 0.55–0.8% than that of ZnO photoanode of 0.28%. The SZO4 photoanode had the highest power energy conversion efficiency (η) of 0.80% with a photocurrent density (J_{sc}) of $2.09\,mA\,cm^{-2}$, an open-circuit voltage (V_{oc}) of 0.57 V, and a fill factor (FF) of 66.9%. SEM micrographs show that the average size of the particles varies with the content of Sn element and the average particle size of SZO4 is smaller than other powders. From the result of dye adsorbed amount on ZnO and SZO photoanodes, which was shown in Table 1, it was found that SZO4 exhibits the highest amount of dye adsorbed of $3.114 \times 10^{-5}\,mM\,cm^{-2}$.

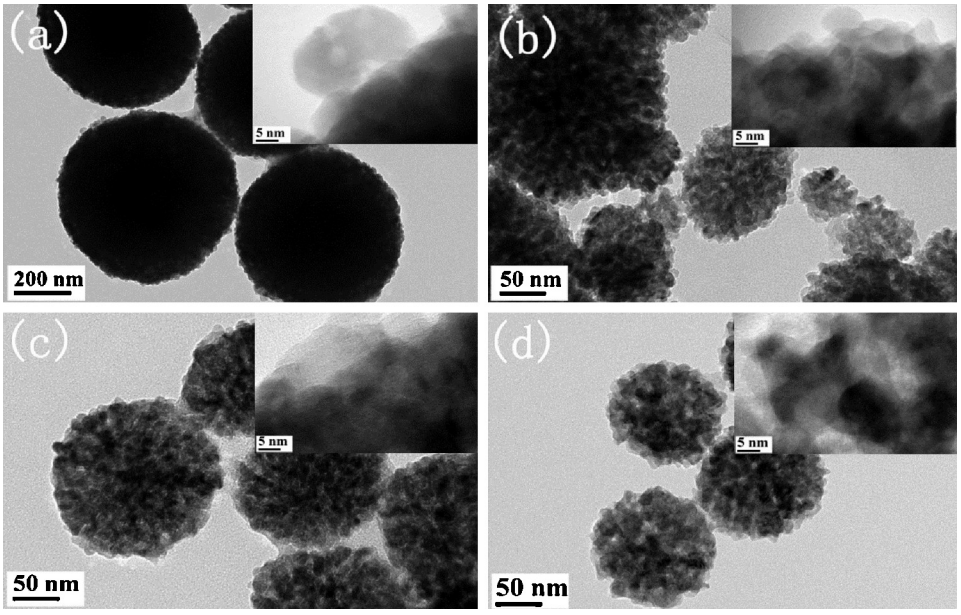

Fig. 3. TEM images of (a) ZnO, (b) SZO3, (c) SZO4, and (d) SZO5 spherical particles. The insets are the corresponding high magnification images.

Table 1
Photovoltaic properties of DSSCs based on ZnO and SZO photoelectrodes.

Photoelectrodes	J_{sc} (mA cm^{-2})	V_{oc} (V)	FF (%)	IPCE (%)	η (%)	Dye adsorbed ($\times 10^{-5}$, mM cm^{-2})
ZnO	0.84	0.59	57.2	17.5	0.28	1.038
SZO3	1.44	0.59	65.1	24.4	0.55	2.595
SZO4	2.09	0.57	66.9	38.4	0.80	3.114
SZO5	1.62	0.59	67.8	34.2	0.66	2.744

Fig. 4(b) displays the wavelength distribution of incident photon to current conversion efficiency (IPCE) of DSSCs based on ZnO and SZO photoanodes. The IPCE shows the wavelength, which around 400–700 nm, is ascribed to the N719 dye. The maximum IPCE value at 515 nm is 17.5, 24.4, 34.5 and 38.4% for ZnO, SZO3, SZO4 and SZO5, respectively. The IPCE (λ) value can be calculated by means of the equation of IPCE (λ) = LHE (λ)$\Phi_{inj}\eta_c$, where LHE (λ) represents the light-harvesting efficiency and is mainly related to the amount of dye adsorption on the surface of photoanode; Φ_{inj} and η_c that are dependent on the photoanode property representing the quantum yield of electron injection from the excited sensitizer to semiconductor and the collection efficiency of injected electrons, respectively [22]. In this study, the LHE (λ) of SZO4 is much higher than other samples due to the high amount of dye adsorption on the surface of SZO nanocrystallites.

To quantify the dye content of the ZnO electrodes, the dye was desorbed into a 1:1 volume of 0.5 M NaOH and ethanol mixture solution and analyzed the solution using the adsorption peak intensity of N719 at 515 nm. The results are presented in Table 1. The dye loading was calculated to be 1.038×10^{-5} mM cm^{-2}, 2.595×10^{-5} mM cm^{-2}, 3.114×10^{-5} mM cm^{-2} and 2.744×10^{-5} mM cm^{-2} for ZnO, SZO3, SZO4 and SZO5 photoelectrodes, respectively. The amount of dye absorbed on the SZO4 photoelectrodes is three times more than that on ZnO photoelectrodes.

3.3. EIS analyses

To reveal the kinetics of electrochemical properties at the interface of nanoparticles, the electrochemical impedance spectroscopy (EIS) of the DSSCs based on ZnO and SZO photoanodes were investigated in a frequency range from 0.1 Hz to 1 MHz. Fig. 5 shows the Nyquist plots obtained by EIS. Two semicircles are observed from the Nyquist plots. According to the EIS model of DSSCs reported

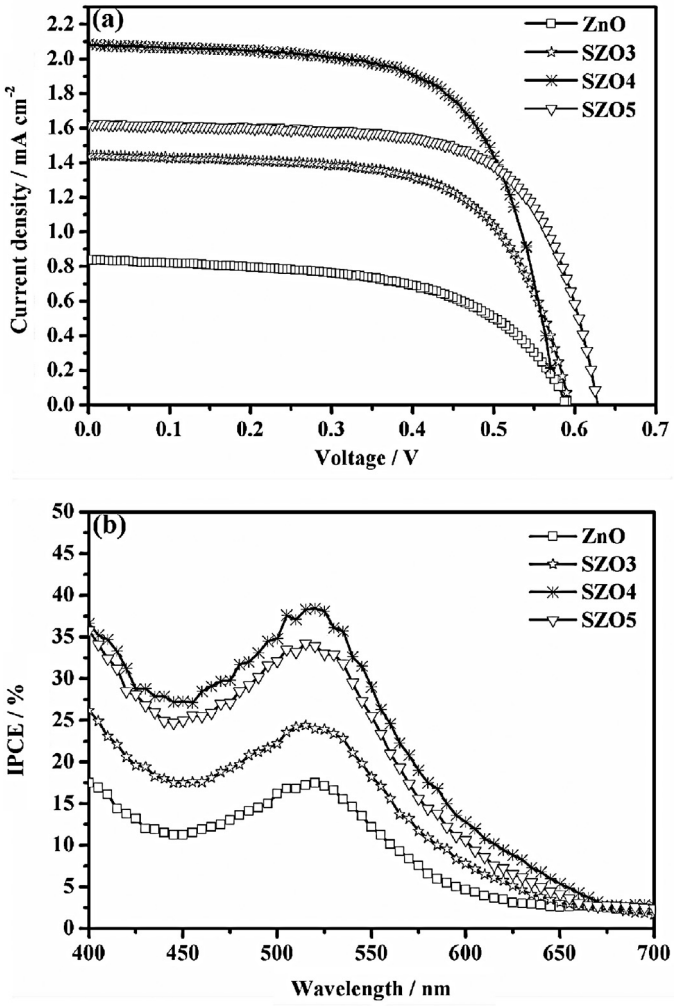

Fig. 4. (a) *J–V* curves and (b) IPCE spectra of DSSCs based on ZnO and SZO photoelectrodes.

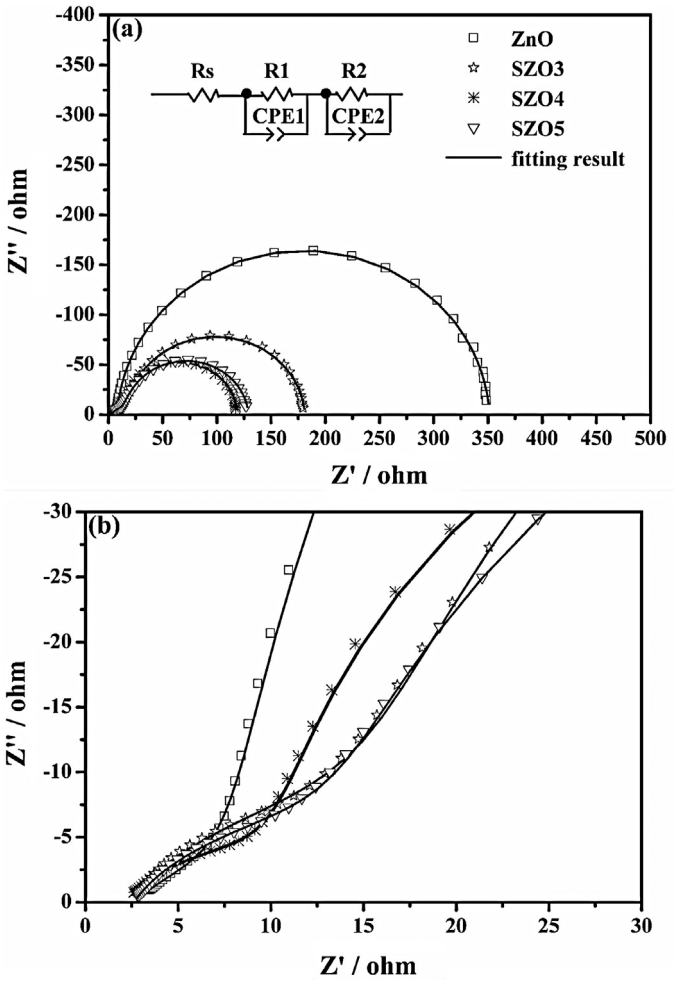

Fig. 5. (a) Typical Nyquist plots of DSSCs based on ZnO and SZO photoelectrodes and the inset is the equivalent circuit model. (b) Zoom in images of typical Nyquist plots in the high-frequency region.

Table 2
The resistances of DSSCs based on ZnO and SZO photoelectrodes.

Devices	R_s (Ω)	R_1 (Ω)	R_2 (Ω)
ZnO	2.7	6.5	342.4
SZO3	2.3	13.6	162.1
SZO4	2.2	9.4	107.4
SZO5	2.6	13.4	113.0

in the literature [23,24], the first semicircle in the high-frequency region represents the resistance applied to the charge transfer at the interfaces of the electrolyte–Pt counter-electrode (R_1). The second semicircle in intermediate frequencies represents the transport resistance of electrons within the photoanode and the charge transfer at the dyed-photoanode–electrolyte (R_2) interface. The R_1 and R_2 are further shunt-wound with a constant phase element (CPE) instead of the chemical capacitance (C_μ) considering the inhomogeneity of its inner surfaces. The resistance of R_s, R_1 and R_2 that are determined by fitting the experimental data according to the equivalent circuit (Fig. 5 inset) were listed in Table 2. R_s represents the resistance of FTO. R_2 in the DSSCs based on ZnO, SZO3, SZO4, and SZO5 is 342.4, 162.1, 107.4 and 113.0 Ω, respectively. SZO4 had the lowest resistance comparing to the other samples; therefore, it exhibited the highest J_{sc} of 2.09 mA cm^{-2} and η of 0.80%.

4. Conclusion

In conclusion, we report the material characteristics and electrochemical performance of the DSSCs based on ZnO and SZO photoanodes. The FE-SEM micrograph shows that the aggregated spherical submicron particles of SZO powders are significantly smaller than that of ZnO, therefore, the SZO photoanodes adsorbed high amount of dye on the surface of SZO photoanodes. The SZO4 (Sn–Zn = 4 wt.%) photoanode yields the highest power energy conversion efficiency (η) of 0.80% with a photocurrent density (J_{sc}) of 2.09 mA cm^{-2}, an open-circuit voltage (V_{oc}) of 0.57 V, a fill factor (FF) of 66.9% due to its lowest resistance and highest amount of dye adsorption.

Acknowledgement

Financial support for this work was provided by the National Science Council of Taiwan under contract No. NSC 99-2221-E-155-028.

References

[1] B. O'Regan, M. Grätzel, A low-cost, high efficiency solar cell based on dye-sensitized colloidal TiO_2 films, Nature 353 (1991) 737.
[2] E. Kaidashev, M. Lorenz, H. Von Wenckstern, A. Rahm, H.C. Semmelhack, K.H. Han, G. Benndorf, C. Bundesmann, H. Hochmuth, M. Grundmann, High electron mobility of epitaxial ZnO thin films on c-plane sapphire grown by multistep pulsed-laser deposition, Appl. Phys. Lett. 82 (2003) 3901.
[3] S. Ameen, M.S. Akhtar, H.K. Seo, Y.S. Kim, H.S. Shin, Influence of Sn doping on ZnO nanostructures from nanoparticles to spindle shape and their photoelectrochemical properties for dye sensitized solar cells, Chem. Eng. J. 187 (2012) 351.
[4] R. Tao, T. Tomita, R.A. Wong, K. Waki, Electrochemical, structural analysis of Al-doped ZnO nanorod arrays in dye-sensitized solar cells, J. Power Sources 214 (2012) 159.
[5] A.S. Gonçalves, M.S. Góes, F.F. Santiago, T. Moehl, M.R. Davolos, J. Bisquert, S. Yanagida, A.F. Nogueira, P.R. Bueno, Doping saturation in dye-sensitized solar cells based on ZnO:Ga nanostructured photoanodes, Electrochim. Acta 56 (2011) 6503.
[6] L. Luo, W. Tao, X. Hu, T. Xiao, B. Heng, W. Huang, H. Wang, H. Han, Q. Jiang, J. Wang, Y. Tang, Mesoporous F-doped ZnO prism arrays with significantly enhanced photovoltaic performance for dye-sensitized solar cells, J. Power Sources 196 (2011) 10518.
[7] A. Tubtimtae, M.W. Lee, ZnO nanorods on undoped and indium-doped ZnO thin films as a TCO layer on nonconductive glass for dye-sensitized solar cells, Superlattices Microstruct. 52 (2012) 987.
[8] B.S. Kang, K.S. Kim, S.C. Yu, H. Chae, First-principles study for ferromagnetism of Cu-doped ZnO with carrier doping, J. Solid State Chem. 198 (2013) 120.
[9] M. Peiteado, Y. Iglesias, J.F. Fernandez, J. De Frutos, A.C. Caballero, Microstructural development of tin-doped ZnO bulk ceramics, Mater. Chem. Phys. 101 (2007) 1.
[10] C.Y. Tsay, H.C. Cheng, Y.T. Tung, W.H. Tuan, C.K. Lin, Effect of Sn-doped on microstructural and optical properties of ZnO thin films deposited by sol–gel method, Thin Solid Films 517 (2008) 1032.
[11] H. Benelmadjat, B. Boudine, O. Halimi, M. Sebais, Fabrication and characterization of pure and Sn/Sb-doped ZnO thin films deposited by sol–gel method, Opt. Laser Technol. 41 (2009) 630.
[12] K.C. Yung, H. Liem, H.S. Choy, Enhanced redshift to the optical band gap in Sn-doped ZnO free standing films using the sol–gel method, J. Phys. D Appl. Phys. 42 (2009) 185002.
[13] I. Gonzalez-Valls, Y. Yu, B. Ballesteros, J. Oro, M. Lira-Cantu, Synthesis conditions, light intensity and temperature effect on the performance of ZnO nanorods-based dye sensitized solar cells, J. Power Sources 196 (2011) 6609.
[14] C. Jiang, X. Sun, G. Lo, D. Kwong, J. Wang, Improved dye-sensitized solar cells with a ZnO-nanoflower photoanode, Appl. Phys. Lett. 90 (2007) 263501.
[15] A.B.F. Martinson, J.W. Elam, J.T. Hupp, M.J. Pellin, ZnO nanotube based dye-sensitized solar cells, Nano Lett. 7 (2007) 2183.
[16] S.H. Ko, D. Lee, H.W. Kang, K.H. Nam, J.Y. Yeo, S.J. Hong, C.P. Grigoropoulos, H.J. Sung, Nanoforest of hydrothermally grown hierarchical ZnO nanowires for a high efficiency dye-sensitized solar cell, Nano Lett. 11 (2011) 666.
[17] I.D. Kim, J.M. Hong, B.H. Lee, D.Y. Kim, E.K. Jeon, D.K. Choi, D.J. Yang, Dye-sensitized solar cells using network structure of electrospun ZnO nanofiber mats, Appl. Phys. Lett. 91 (2007) 163109.
[18] Q. Zhang, G. Cao, Hierarchically structured photoelectrodes for dye-sensitized solar cells, J. Mater. Chem. 21 (2011) 6769.
[19] Y.J. Kim, M.H. Lee, H.J. Kim, G. Lim, Y.S. Choi, N.G. Park, K. Kim, W.I. Lee, Formation of highly efficient dye-sensitized solar cells by hierarchical pore generation with nanoporous TiO_2 spheres, Adv. Mater. 21 (2009) 3668.
[20] D. Jezequel, J. Guenot, N. Jouini, F. Fievet, Submicrometer zinc oxide particles: elaboration in polyol medium and morphological characteristics, J. Mater. Res. 10 (1995) 77.
[21] Q. Zhang, T.P. Chou, B. Russo, S.A. Jenekhe, G. Cao, Polydisperse aggregates of ZnO nanocrystallites: a method for energy-conversion-efficiency enhancement in dye-sensitized solar cells, Adv. Funct. Mater. 18 (2008) 1654.
[22] Q. Zhang, T.P. Chou, B. Russo, S.A. Jenekhe, G. Cao, Aggregation of ZnO nanocrystallites for high conversion efficiency in dye-sensitized solar cells, Angew. Chem. 120 (2008) 2436.
[23] M.H. Jung, H.G. Yun, S. Kim, M.G. Kang, ZnO nanosphere fabrication using the functionalized polystyrene nanoparticles for dye-sensitized solar cells, Electrochim. Acta 55 (2010) 6563.
[24] Q. Wang, J.E. Moser, M. Grätzel, Electrochemical impedance spectroscopic analysis of dye-sensitized solar cells, J. Phys. Chem. B 109 (2005) 14945.